Inorg. Chem. **2002**, *41*, 3521–3527

Tetrakis(*N*,*N*′-dimethylbenzamidinato)diruthenium(III) Compounds Bearing Axial Chloro and Alkynyl Ligands: A New Family of Redox Rich Diruthenium Compounds

Guolin Xu,[†] Charles Campana,[‡] and Tong Ren*,[†]

Department of Chemistry and Center for Supramolecular Science, University of Miami, Coral Gables, Florida 33124, and Bruker AXS Inc., Madison, Wisconsin 53711

Received January 28, 2002

Novel diruthenium(III) compound $Ru_2(DMBA)_4Cl_2$ (**1**, DMBA = *N*,*N*′-dimethylbenzamidinate) was obtained via refluxing $Ru_2(OAc)_4Cl$ with dimethylbenzamidine in the presence of LiCl and Et_3N under ambient atmosphere. Metathesis reactions between **1** and MC_2Y (M = Li and Na) yielded bis-alkynyl derivatives $Ru_2(DMBA)_4(C_2Y)_2$ (Y = $SiMe_3$ (**2a**), H (**2b**), Ph (**2c**), and C_2SiMe_3 (**3a**)), and further desilylation of **3a** using K_2CO_3 resulted in $Ru_2(DMBA)_4(C_4H)_2$ (**3b**). Compound **1** is paramagnetic ($S = 1$), while compounds **2** and **3** are diamagnetic. The single-crystal X-ray diffraction study revealed that the Ru–Ru distances are 2.3224(7), 2.4501(6), and 2.4559(6) Å for **1**, **2a**, and **3b**, respectively. A strong Ru–C σ-bond in alkynyl adducts was implied by the short Ru–C distances in **2a** (1.955(4) Å) and **3b** (1.952[5] Å). All the compounds undergo three one-electron redox processes, an oxidation and two reductions, and the reversibility of redox couples depends on the nature of axial ligands.

Introduction

Within the family of established metal−metal bonded dinuclear species, diruthenium paddlewheel compounds distinguish themselves with both the rich redox chemistry and diversified magneto- and spectroscopic features.[1] The latter have provided ample opportunity for probing the intricate manifolds of electronic configurations of M−M bonded dinuclear species.[2] There has been a recent surge of interest in incorporating diruthenium paddlewheel compounds into various supramolecular constructs. Utilizing various organonitrogen bridging ligands, diruthenium carboxylates have been incorporated into both one-dimensional chains[3−6] and two-dimensional networks,[7] where moderate interdimer magnetic couplings have been observed. Much enhanced interdimer electronic couplings have been observed recently between two diruthenium units bridged by polyynediyl (C_{2m}^{2-}) linkers in both ours[8] and Lehn's laboratories,[9] and the possibility of realizing molecular electronic wires based on these linked diruthenium units has been proposed (Scheme 1).[10−12]

Scheme 1. Oligo-metalla-yne Wires Based on Ru_2 Compound[a]

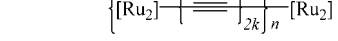

[a] *k*, *n* = integers.

To achieve the oligomer outlined in Scheme 1, a difunctional module *trans*-{$YC_{2k}-Ru_2-C_{2k}Y$}, where Y is either R_3Si or H, is required from the structural consideration. Our previous work in developing difunctional modules was based on two sets of supporting ligands (Scheme 2): diarylformamidinates (DArF) and 2-anilinopyridinate (ap).[10,11,13] In both

* To whom correspondence should be addressed. E-mail: tren@miami.edu. Phone: (305) 284-6617. Fax: (305) 284-1880.
[†] University of Miami.
[‡] Bruker AXS Inc.

(1) Cotton, F. A.; Walton, R. A. *Multiple Bonds between Metal Atoms*; Oxford University Press: Oxford, 1993.
(2) Miskowski, V. M.; Hopkins, M. D.; Winkler, J. R.; Gray, H. B. In *Inorganic Electronic Structure and Spectroscopy*; Solomon, E.I., Lever, A. B. P., Eds.; Wiley: New York, 1999; Vol. 2.
(3) Cotton, F. A.; Kim, Y.; Ren, T. *Inorg. Chem.* **1992**, *31*, 2723.
(4) Handa, M.; Sayama, Y.; Mikuriya, M.; Nukada, R.; Hiromitsu, I.; Kasuga, K. *Bull. Chem. Soc. Jpn.* **1998**, *71*, 119.
(5) Miyasaka, H.; Clérac, R.; Campos-Fernández, C. S.; Dunbar, K. R. *J. Chem. Soc., Dalton Trans.* **2001**, 858.
(6) Miyasaka, H.; Clérac, R.; Campos-Fernández, C. S.; Dunbar, K. R. *Inorg. Chem.* **2001**, *40*, 1663.
(7) Miyasaka, H.; Campos-Fernández, C. S.; Clérac, R.; Dunbar, K. R. *Angew. Chem., Int. Ed.* **2000**, *39*, 3831.
(8) Ren, T.; Zou, G.; Alvarez, J. C. *Chem. Commun.* **2000**, 1197.
(9) Wong, K.-T.; Lehn, J.-M.; Peng, S.-M.; Lee, G.-H. *Chem. Commun.* **2000**, 2259.
(10) Xu, G.; Ren, T. *Organometallics* **2001**, *20*, 2400.
(11) Xu, G.; Ren, T. *Inorg. Chem.* **2001**, *40*, 2925.
(12) Ren, T. *Organometallics* **2002**, *21*, 732.
(13) Zou, G.; Alvarez, J. C.; Ren, T. *J. Organomet. Chem.* **2000**, *596*, 152.

10.1021/ic0200794 CCC: $22.00
Published on Web 05/23/2002

Scheme 2. Diarylformamidinate and 2-Anilinopyridinate Ligands

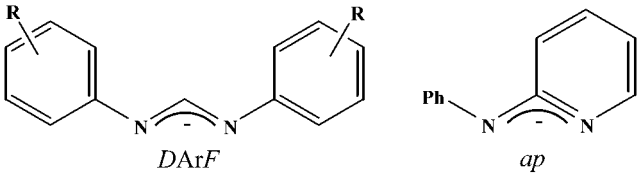

cases, the presence of aryl groups that flank either one or both axial positions of the Ru_2 core necessitates the use of butadiynyl or longer alkynyl ligand ($k \geq 2$) in realizing the difunctional module. Consequently, oligomer **A** based on these modules will have a polyyne-diyl bridge with a minimum of four C≡C bonds. Because the electronic coupling generally decays exponentially as the length of the bridge increases,[14] use of shorter polyyne-diyl bridges is desired for achieving a higher degree of electronic delocalization. Hence, achieving difunctional modules bearing axial ethynyl ligands is very significant in this regard. *N*,*N*′-Dimethylbenzamidinate (DMBA), a ligand previously used in supporting both the Cr_2 and Fe_2 cores,[15,16] appears to exert a minimum steric effect around the axial positions and hence is appealing for the ethynyl-based difuctional modules. Described in this contribution are the synthesis and characterizations of the novel diruthenium(III,III) compound $Ru_2(DMBA)_4Cl_2$ (**1**), and its bis(ethynyl) (**2**) and bis(butadiynyl) (**3**) derivatives (Scheme 3).

Scheme 3. DMBA-Bridged Diruthenium Compounds

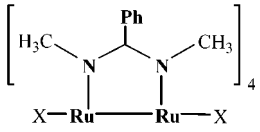

X = Cl (**1**); C_2SiMe_3(**2a**) , C_2H (**2b**), C_2Ph (**2c**); C_4SiMe_3 (**3a**), C_4H (**3b**)

Results and Discussion

Hoping to obtain a $Ru_2^{(II,III)}L_4Cl$ type compound based on the DMBA bridge, we used the same synthetic procedure as that described for $Ru_2(DArF)_4Cl$:[17] refluxing $Ru_2(OAc)_4Cl$ with 5 equiv of HDMBA in the presence of Et_3N and LiCl under an ambient atmosphere. However, $Ru_2(DMBA)_4Cl_2$, a $Ru_2^{(III,III)}$ species, was isolated in a nearly quantitative yield. The formulation is supported by both the FAB-mass datum and combustion analysis of the chlorine content, and the X-ray single-crystal structure study. Clearly, *N*,*N*′-dimethylbenzamidinate is a much stronger donor than *N*,*N*′-diarylformamidinates because of the difference in N-substituent, and the enhanced electron richness stabilizes the Ru_2(III,III) core instead of the Ru_2(II,III) core. This is also consistent with the report of Bear et al. that treating $Ru_2(OAc)_4Cl$ with Hhpp (1,3,4,6,7,8-hexahydro-2*H*-pyrimido-[1,2-*a*]pyrimidine) under molten conditions resulted in $Ru_2(hpp)_4Cl_2$ in 40% yield.[18] Compound **1** is paramagnetic and has a room-temperature magnetic moment of 2.86 μ_B, indicating an $S = 1$ ground state similar to that of $Ru_2(hpp)_4Cl_2$.

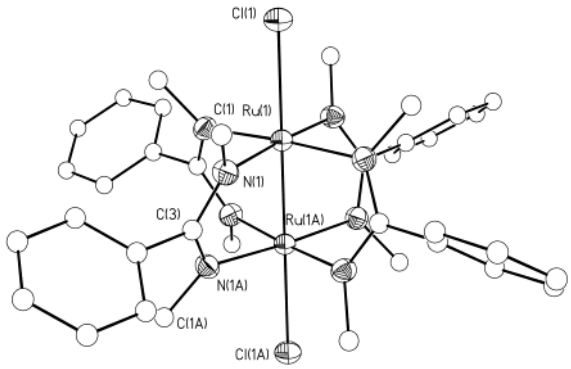

Figure 1. ORTEP plot of molecule **1** at 30% probability level.

Previous work demonstrated that both the mono- and bis-alkynyl adducts of diruthenium core can be prepared from the reaction between Ru_2L_4Cl (L = DArF, ap, and 2-perfluoroanilinopyridinate) and LiC_2Y, depending on the nature of Y and stoichiometry of lithiated alkynyl.[10−13,19−23] In contrast, the bis-alkynyl adduct is the only product isolated with all C_2Y (Y = H, $SiMe_3$, Ph, C_2SiMe_3) ligands employed in this study. An attempt to isolate the monosubstituted species (YC_2−[Ru_2L_4]−Cl) by treating **1** with 1 equiv of alkynyl ligand resulted in the bis-adduct along with unreacted **1**. A plausible explanation is that the binding of the first alkynyl ligand to $Ru_2(DMBA)_4$ core induces an accelerated addition of the second alkynyl. However, the origin of such a synergetic effect remains unclear. To maximize the yield of **2**/**3**, 5 equiv of alkynyl ligand were used in all the syntheses. Interestingly, the metathesis reaction between $Ru_2(hpp)_4Cl_2$ and lithiated alkynyl failed to yield any kind of alkynyl adducts, which was attributed to the substitution of the bridging hpp by the alkynyl ligand.[18]

Compound **2a** is the first example of bis(trimethylsilylacetylide) adduct on a Ru_2 core, confirming the minimized steric effect around both axial positions. It is interesting to note that the attempted desilylation of **2a** using either Bu_4NF (in THF with 5% H_2O) or K_2CO_3 failed to yield **2b**. Failure of direct desilylation of metal-bound trimethylsilylacetylide has also been noted for mononuclear Mn and Nb complexes[24,25] and is attributed to a reduced nucleophilicity

(14) Launay, J.-P. *Chem. Soc. Rev.* **2001**, *30*, 386.
(15) Bino, A.; Cotton, F. A.; Kaim, W. *Inorg. Chem.* **1979**, *18*, 3566.
(16) Cotton, F. A.; Daniels, L. M.; Matonic, J. H.; Murillo, C. A. *Inorg. Chim. Acta* **1997**, *256*, 277.
(17) Lin, C.; Ren, T.; Valente, E. J.; Zubkowski, J. D.; Smith, E. T. *Chem. Lett.* **1997**, 753.
(18) Bear, J. L.; Li, Y.; Han, B.; Caemelbecke, E. V.; Kadish, K. M. *Inorg. Chem.* **1996**, *35*, 3053.
(19) Bear, J. L.; Han, B.; Huang, S. *J. Am. Chem. Soc.* **1993**, *115*, 1175.
(20) Bear, J. L.; Han, B.; Huang, S.; Kadish, K. M. *Inorg. Chem.* **1996**, *35*, 3012.
(21) Bear, J. L.; Li, Y.; Han, B.; Caemelbecke, E. V.; Kadish, K. M. *Inorg. Chem.* **1997**, *36*, 5449.
(22) Lin, C.; Ren, T.; Valente, E. J.; Zubkowski, J. D. *J. Chem. Soc., Dalton Trans.* **1998**, 571.
(23) Lin, C.; Ren, T.; Valente, E. J.; Zubkowski, J. D. *J. Organomet. Chem.* **1999**, *579*, 114.
(24) Fernandez, F. J.; Alfonso, M.; Schmalle, H. W.; Berke, H. *Organometallics* **2001**, *20*, 3122.
(25) García-Yebra, C.; López-Mardomingo, C.; Fajardo, M.; Antiñolo, A.; Otero, A.; Rodríguez, A.; Vallat, A.; Lucas, D.; Mugnier, Y.; Carbó, J. J.; Lledós, A.; Bo, C. *Organometallics* **2000**, *19*, 1749.

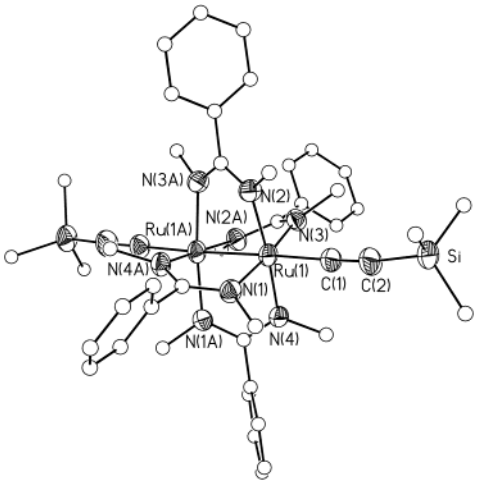

Figure 2. ORTEP plot of molecule **2a** at 30% probability level.

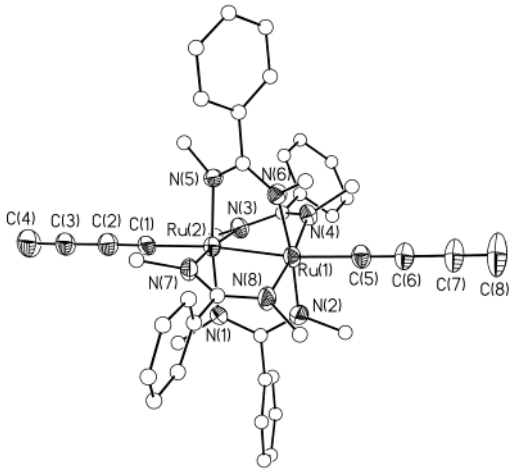

Figure 3. ORTEP plot of molecule **3b** at 30% probability level.

of F^- in the presence of water. Nevertheless, compound **2b** can be prepared directly from the reaction between **1** and NaCCH. On the other hand, compound **3a** is readily converted to **3b** by K_2CO_3, a mild desilylation agent. The difference in reactivity between **2a** and **3a** is clearly electronic: butadiynyl ligand is more electron-deficient and consequentially more susceptible to nucleophilic desilylation reaction. This is also consistent with our previous observation that the desilylation occurs first at the butadiynyl end in *trans*-$(Me_3SiC_4)[Ru_2(ap)_4](C_2SiMe_3)$.[12] Both compounds **2** and **3** are diamagnetic and exhibit well-resolved ^1H and ^{13}C NMR spectra.

Molecular structures of compounds **1**, **2a**, and **3b** have been established by single-crystal X-ray diffraction studies, and structural plots are shown in Figures 1−3, respectively. It is clear that DMBA ligand adopts the expected *N*,*N*′-bidentate bridging coordination mode and the diruthenium core has the classical paddlewheel coordination motif.[1] In this motif, two chloro/alkynyl ligands occupy the opposite axial positions and are approximately collinear with the Ru−Ru vector. Selected bond lengths and angles around diruthenium core are compiled in Table 1 for all three compounds.

Molecule **1** has a point symmetry group D_4 imposed by the space group *I*422 with the principal C_4 axis coinciding with the Cl1−Ru1−Ru1A−Cl1A vector. Both the Ru−Ru (2.3224(7) Å) and Ru−N bond lengths (2.042(2) Å) in **1** are identical to that of $Ru_2(hpp)_4Cl_2$ (2.321(1) and 2.045(5) Å) within experimental errors.[26] The Ru−Cl bond (2.557(1) Å) is shorter than that of $Ru_2(hpp)_4Cl_2$ (2.705 Å) but is significantly longer than those found for $Ru_2(DArF)_4Cl$ (2.412−2.433 Å).[17,20,27] Similarity in both the structure and magnetism between **1** and $Ru_2(hpp)_4Cl_2$ clearly indicates that they are isoelectronic. Likely, the ground-state configuration of compound **1** is $\sigma^2\pi^4\delta^2\pi^{*2}$, which implies a Ru−Ru bond order of 3 for **1**.[28]

The Ru−Ru distances in **2a** (2.4501(6) Å) and **3b** (2.4559(6) Å) are nearly identical and comparable with those reported for bis(alkynyl) adducts on a $Ru_2(ap)_4$ core (2.450−2.475 Å)[10,12,21] but shorter than those of a $Ru_2(DArF)_4$ core (2.506−2.599 Å, see Table 2).[11,20,22] Both the elongated Ru−Ru bond relative to the parent compound and diamagnetism indicate that all the bis(alkynyl) adducts are isoelectronic. The Ru−C_α distance is about 1.95 Å in both **2a** and **3b**, indicating a strong Ru−C σ bond. Consequently, there is no net Ru−Ru σ-bond, and the ground-state configuration of both **2** and **3** is best described as $\pi^4\delta^2\pi^{*4}$.[28] For the purpose of comparison, key bond lengths and angles around Ru_2 core have been collected in Table 2 for the known bis(alkynyl) adducts.

Significant deviation from an effective D_4 symmetry in the first coordination sphere of Ru_2 core has been observed in compounds of general formula *trans*-$Ru_2L_4(C_2Y)_2$[10−12,20−22,31] and was attributed to a second-order Jahn−Teller distortion on the basis of Fenske−Hall type MO calculations.[22] The structural distortion also occurs in **2a** and **3b**, albeit in different degrees. Among four independent Ru−N bonds in **2a**, there are clearly two short (Ru(1)−N(1) and Ru(1)−N(2)) and two long (Ru(1)−N(3) and Ru(1)−N(4)), but the difference between the longest and shortest Ru−N bond is small (0.041 Å). The distortion becomes more pronounced in **3b**: there is a pair of trans nitrogen centers on each Ru center exhibiting compressed and stretched Ru−N bonds (N(4) and N(8) on Ru(1), and N(3) and N(7) on Ru(2)), and the Ru−N bond length ranges from 1.993(4) to 2.107(4) Å. It is clear from Table 2 that molecule **2a** has the least distortion among all known *trans*-$Ru_2L_4(C_2Y)_2$ type compounds. It is possible that the second-order Jahn−Teller distortion in **2a** is partially suppressed by the steric repulsion between the Me_3Si and *N*-Me groups. A similar effect was observed in the case of *trans*-$(Me_3SiC_4)[Ru_2(ap)_4](C_2Si^iPr_3)$.[12] As elaborated previously,[22] the second-order Jahn−Teller distortion is a global structural effect, and it is also reflected by the significant deviation of the Ru−Ru−C angle from linearity. The majority of bis-alkynyl adducts tabulated have a deviation of 10° or more, while **2a** has an exceptionally small 5° deviation that is consistent with the suppressed distortion.

(26) Bear, J. L.; Li, Y.; Han, B.; Kadish, K. M. *Inorg. Chem.* **1996**, *35*, 1395.
(27) Cotton, F. A.; Ren, T. *Inorg. Chem.* **1995**, *34*, 3190.
(28) Cotton, F. A.; Yokochi, A. *Inorg. Chem.* **1997**, *36*, 567.

Table 1. Selected Bond Lengths (Å) and Angles (deg) for Compounds **1**, **2a**, and **3b**

1		**2a**		**3b**			
Ru(1)−Ru(1A)	2.3228(6)	Ru(1)−Ru(1A)	2.4501(6)	Ru(1)−Ru(2)	2.4559(6)	Ru(1)−C(5)	1.949(5)
Ru(1)−N(1)	2.042(2)	Ru(1)−N(1)	2.026(3)	Ru(1)−N(8)	1.993(4)	Ru(2)−C(1)	1.954(5)
Ru(1)−Cl(1)	2.557(1)	Ru(1)−N(2)	2.028(3)	Ru(1)−N(2)	2.034(4)	C(1)−C(2)	1.203(6)
N(1)−C(1)	1.470(3)	Ru(1)−N(3)	2.062(3)	Ru(1)−N(6)	2.047(4)	C(2)−C(3)	1.361(7)
N(1)−C(3)	1.335(2)	Ru(1)−N(4)	2.067(3)	Ru(1)−N(4)	2.107(4)	C(3)−C(4)	1.178(9)
		Ru(1)−C(1)	1.955(4)	Ru(2)−N(3)	1.998(4)	C(5)−C(6)	1.212(6)
		C(1)−C(2)	1.207(6)	Ru(2)−N(5)	2.021(3)	C(6)−C(7)	1.373(7)
		Si−C(2)	1.783(5)	Ru(2)−N(1)	2.063(4)	C(7)−C(8)	1.159(9)
				Ru(2)−N(7)	2.093(4)		
N(1)−Ru(1)−Ru(1A)	88.20(5)	C(1)−Ru(1)−Ru(1A)	174.8(1)	C(5)−Ru(1)−Ru(2)	170.3(1)	C(1)−Ru(2)−Ru(1)	170.7(1)
C(3)−N(1)−Ru(1)	119.2(2)	N(1)−Ru(1)−Ru(1A)	88.79(10)	N(8)−Ru(1)−Ru(2)	92.48(12)	N(3)−Ru(2)−Ru(1)	92.34(12)
N(1)−C(3)−N(1A)	118.6(3)	N(2)−Ru(1)−Ru(1A)	88.88(10)	N(2)−Ru(1)−Ru(2)	87.89(12)	N(5)−Ru(2)−Ru(1)	87.63(11)
		N(3)−Ru(1)−Ru(1A)	84.30(9)	N(6)−Ru(1)−Ru(2)	85.49(11)	N(1)−Ru(2)−Ru(1)	85.49(12)
		N(4)−Ru(1)−Ru(1A)	83.90(9)	N(4)−Ru(1)−Ru(2)	80.54(11)	N(7)−Ru(2)−Ru(1)	81.27(11)
		C(2)−C(1)−Ru(1)	176.6(5)	C(6)−C(5)−Ru(1)	176.7(5)	C(2)−C(1)−Ru(2)	177.7(5)
		C(1)−C(2)−Si	170.9(5)				
N(1)−Ru(1)−Ru(1A)−N(1A)	19.0(2)	N(4)−Ru(1)−Ru(1A)−N(1A)	19.70(15)	N(2)−Ru(1)−Ru(2)−N(1)	17.87(15)	N(6)−Ru(1)−Ru(2)−N(5)	17.72(14)
		N(3)−Ru(1)−Ru(1A)−N(2A)	19.10(14)	N(4)−Ru(1)−Ru(2)−N(3)	18.16(14)	N(8)−Ru(1)−Ru(2)−N(7)	17.12(16)

Table 2. Comparison of Key Structural Parameters among *trans*-$Ru_2L_4(CCY)_2$

L	Y	Ru−Ru	Ru−C	Ru−N_{av} (Δ_{max}[a])	Ru−Ru−C
DPhF[b]	Ph	2.558	1.987	2.054 (0.103)	160
DpClPhF[c]	Ph	2.555	1.991	2.054 (0.099)	159
F_5ap[d]	Ph	2.441	1.955, 1.951	2.068 (0.091)	171, 172
ap[e]	Ph	2.471	1.987, 1.989	2.062 (0.195)	162, 164
DmAnF[f]	C_2SiMe_3	2.599	1.947	2.056 (0.114)	164
ap[10]	C_2SiMe_3	2.472	1.938, 1.956	2.037 (0.176)	163, 164
DMBA[g]	$SiMe_3$	2.450	1.955	2.046 (0.041)	175
DMBA[g]	C_2SiMe_3	2.456	1.949, 1.954	2.045 (0.114)	170, 171
DMBA[h]	Fc	2.439	1.981, 1.977	2.042 (0.132)	168, 170

[a] Δ_{max} = largest discrepancy among Ru−N bond lengths. [b] DphF is diphenylformamidinate.[20] [c] DpClPhF is di(*p*-Clphenyl)formamidinate.[22] [d] F_5ap is 2-pentafluoroanilinopyridinate, (4,0) isomer listed.[21] [e] ap is 2-anilinopyridinate.[29] [f] DmAnF is di(*m*-methoxyphenyl)formamidinate.[11] [g] This work. [h] Fc is ferrocenyl.[30]

All the compounds reported herein are highly redox active, as shown by their cyclic voltammograms recorded in THF versus Ag/AgCl (Figure 4, Table 3). Compound **1** exhibits three one-electron processes, a quasireversible oxidation at 1.063 V (A), a reversible reduction at −0.321 V (B), and an irreversible reduction at −1.119 V (C), and their designations are outlined in Scheme 4. Couples A and B were also observed for $Ru_2(hpp)_4Cl_2$ at 0.457 and −0.60 V versus SCE, respectively.[18] The significant anodic shift of redox potentials of **1** in comparison with $Ru_2(hpp)_4Cl_2$ clearly indicates that DMBA is not as electron-rich as hpp. Yet, DMBA is a much stronger donor than both DArFs and ap ligands, because the Ru_2^{6+}/Ru_2^{5+} couples (B) in the diruthenium compounds supported by the latter ligands were observed in a more positive potential window of 0.520−1.212 V.[13,17] The irreversibility of second reduction C is likely attributed to the fast dissociation of axial chloro ligand upon reduction, similar to the ECE process associated with the (0/−1) couple in the $Ru_2(DArF)_4Cl$ family.[17,20] However, the oxidation wave of $\{[Ru_2(DMBA)_4]Cl\}^{1-}$ (D) was not observed.

The bis-alkynyl derivatives **2**/**3** exhibit rich redox characteristics similar to that of the parent molecule **1**: all the cyclic voltammograms consist of one one-electron oxidation and at least one one-electron reduction. The oxidation couple

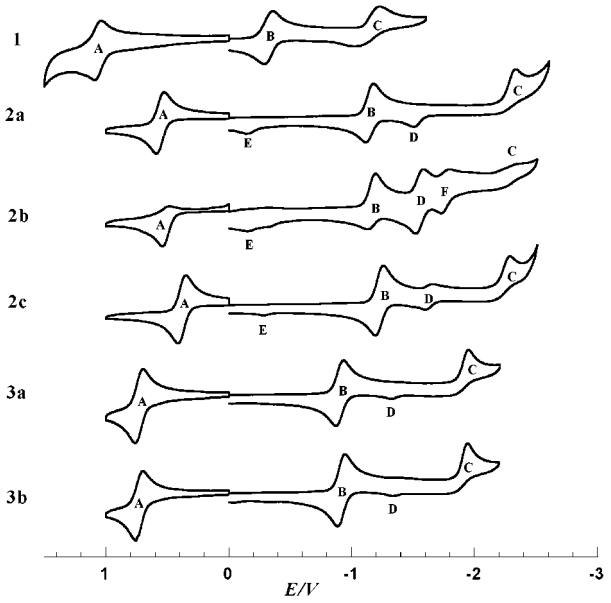

Figure 4. Cyclic voltammograms of compounds **1**−**3** recorded in 0.20 M THF solution of Bu_4NPF_6 at a scan rate of 0.10 V/s.

(A) and first reduction couple (B) of ethynyl adducts **2a**−**c** have been cathodically shifted from those of **1** by ∼0.5 and 0.8 V, respectively, which is clearly attributed to the strong donor nature of the ethynyl ligands in comparison with Cl^-. Similarly, the oxidation couple (A) and first reduction couple (B) of butadiynyl adducts **3a/b** have been respectively shifted from **1** by ∼0.3 and 0.6 V. The smaller potential shifts observed for **3a**/**b** are consistent with the fact that butadiynyl is more electron-deficient than ethynyl ligand.[10,12]

Redox behavior of alkynyl (C_2R and C_4R) derivatives depends on the nature of R. Among the ethynyl compounds, **2a** exhibits a reversible oxidation (A) and a reversible reduction (B) if cathodic sweep is limited within −1.60 V. Extending the window of the cathodic sweep to −2.50 V reveals the second reduction (C). However, the corresponding anodic wave was absent in the backward sweep, and two small, but significant, waves appeared at more positive potentials. As outlined in Scheme 4, the irreversibility of

Table 3. Electrochemical and Spectroscopic Data of Compounds **1**−**3**

	1	**2a**	**2b**	**2c**	**3a**	**3b**
$E(+1/0)$/V	1.063	0.558	0.574[a]	0.517	0.730	0.725
(ΔE_p/V, $i_{back}/i_{forward}$)	(0.044, 0.79)	(0.064, 0.96)		(0.058, 0.89)	(0.069, 0.99)	(0.058, 0.84)
$E(0/-1)$/V	−0.321	−1.141	−1.199[b]	−1.100	−0.897	−0.919
(ΔE_p/V, $i_{back}/i_{forward}$)	(0.073, 0.91)	(0.063, 0.67)		(0.057, 0.79)	(0.058, 0.94)	(0.063, 0.93)
$E(-1/-2)$/V	−1.119	−2.324[b]	−2.276[b]	−2.198[b]	−1.940[b]	−1.945[b]
(ΔE_p/V, $i_{back}/i_{forward}$)	(0.202, 0.33)					
λ_{max}/nm, (ϵ, cm^{-1} M^{-1})	738 (1738)	872 (2410)	858 (2146)	889 (2105)	884 (2220)	876 (2316)
	502 (sh)	580 (sh)	580 (sh)	586 (sh)	580 (sh)	580 (sh)
	426 (3311)	492 (14325)	487 (10508)	501 (14115)	512 (12865)	506 (11969)
$E(+1/0) - E(0/-1)$, V	1.384	1.702	1.773	1.617	1.627	1.644
E_{op}, eV	1.68	1.42	1.45	1.39	1.40	1.42

[a] Irreversible couple, E_{pa} is reported. [b] Irreversible couple, E_{pc} is reported.

Scheme 4. Redox Steps and Related Chemical Steps in $Ru_2(DMBA)_4X_2$ (X = Cl and Alkynyl)

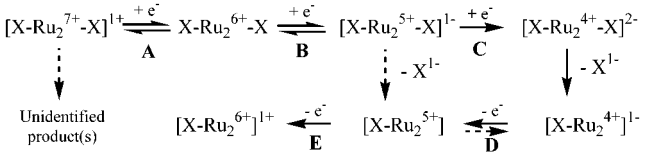

the C couple is possibly due to the fast dissociation of one of two $(C_2SiMe_3)^{1-}$ ligands, and the resultant species $\{[Ru_2(DMBA)_4](C_2SiMe_3)\}^{1-}$ undergoes two consecutive one-electron oxidations (indicated by D and E) during the backward sweep. The CV of phenylethynyl adduct **2c** is similar to that of **2a** except that there is a small but significant wave immediately following wave B during the forward sweep of cathodic scan. This additional feature is attributed to the partial dissociation of phenylethynyl upon the first reduction, revealing that **2c** is less stable toward reduction than **2a**. The removal of Me_3Si from **2a** drastically reduces the redox stability of the ethynyl adduct, as shown by the CV of **2b**, where all the couples became irreversible. The dissociation of ethynyl ligand is so fast that the reduction wave of mono-ethynyl species (D) became very pronounced while the second reduction of the bis-species (C) was barely detectable. There is also an additional wave (F) immediately following D that is unique to **2c**, and its nature has not been resolved. Upon increasing the scan rate (see Support Information for details), the oxidation couple A became quasireversible, while the main feature of the cathodic scan remains the same.

Both butadiynyl adducts **3a** and **3b** are more stable toward redox processes: the oxidation and first reduction couples are reversible, and there is no small wave immediately following the first reduction that is indicative of the alkynyl dissociation. However, the second reduction is irreversible in both cases. Apparently, the strong donor nature of DMBA destabilizes the highly reduced Ru_2 species, and the instability was relieved by the loss of alkynyl anions.

Both parent compound **1** and bis-alkynyl derivatives **2** and **3** feature two major peaks in their vis−NIR spectra, as shown in Figure 5. Two peaks of modest intensity were observed for **1** at 438 and 726 nm, and both are likely charge-transfer transitions: the former as n(Cl) to $\pi^*/\delta^*(Ru_2)$ and the latter as π(Ru−N) to $\pi^*/\delta^*(Ru_2)$.[2] Upon the formation of bis-(alkynyl) adducts **2** and **3**, these charge-transfer bands

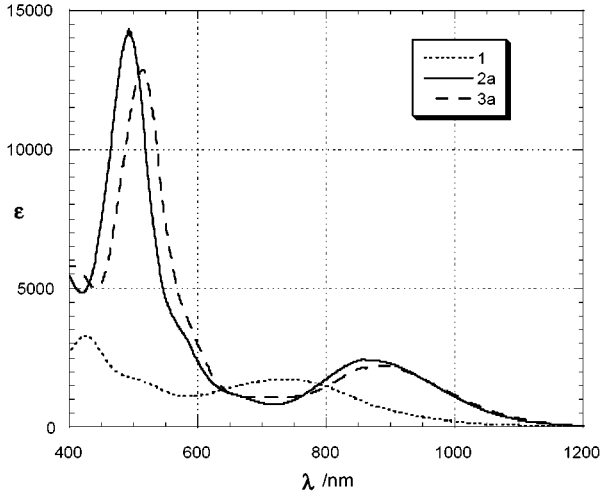

Figure 5. Visible−near-infrared (vis−NIR) spectra of compounds **1**, **2a**, and **3a** recorded in THF.

became intensified and red-shifted to ∼490 and 860 nm, respectively.

Conclusion

The strong donor nature of DMBA permits the isolation of $Ru_2(DMBA)_4Cl_2$ instead of the anticipated $Ru_2(DMBA)_4$-Cl. In contrast with $Ru_2(hpp)_4Cl_2$, $Ru_2(DMBA)_4Cl_2$ undergoes a smooth metathesis reaction with MC_2Y to yield a number of bis-alkynyl derivatives. As evidence of the reduced steric crowding around axial positions, the first bis-trimethylsilyl-ethynyl adduct on a Ru_2 core has been isolated. Currently, we are exploring the oxidative coupling chemistry of these bis-alkynyl building blocks.

Experimental Section

1,4-Bistrimethylsilyl-1,3-butadiyne, sodium acetylide suspension in mineral oil, phenylacetylene, trimethylsilylacetylene, and *n*-BuLi were purchased from Aldrich, Bu_4NF (in THF) was purchased from ACROS, and silica gel was purchased from Merck. $Ru_2(OAc)_4$-Cl[32] and *N*,*N*′-dimethylbenzamidine[15] were prepared as previously described. THF was distilled over Na/benzophenone under an N_2 atmosphere prior to use. ^1H and ^{13}C NMR spectra were recorded

(29) Xu, G.; Ren, T. *J. Organomet. Chem.*, in press.
(30) Xu, G.; DeRosa, M.; Crutchley, R. J.; Ren, T. *J. Am. Chem. Soc.*, manuscript in preparation.
(31) Ren, T. *Coord. Chem. Rev.* **1998**, *175*, 43.
(32) Stephenson, T. A.; Wilkinson, G. *J. Inorg. Nuclear Chem.* **1966**, *28*, 2285.

on a Bruker AVANCE300 NMR spectrometer, with chemical shifts (δ) referenced to the residual $CHCl_3$ and the solvent $CDCl_3$, respectively. Infrared spectra were recorded on a Perkin-Elmer 2000 FT-IR spectrometer using KBr disks. UV−vis spectra in THF were obtained with a Perkin-Elmer Lambda-900 UV−vis spectrophotometer. Magnetic susceptibility was measured at 294 K with a Johnson Matthey Mark-I magnetic susceptibility balance. Elemental analysis was performed by Atlantic Microlab, Norcross, Georgia. Cyclic voltammograms were recorded in 0.2 M $(n\text{-}Bu)_4N\ PF_6$ solution (THF, N_2-degassed) on a CHI620A voltammetric analyzer with a glassy carbon working electrode (diameter = 2 mm), a Pt-wire auxiliary electrode, and a Ag/AgCl reference electrode. The concentration of diruthenium species is always 1.0 mM. The ferrocenium/ferrocene couple was observed at 0.573 V (vs Ag/AgCl) at the experimental conditions.

Preparation of $Ru_2(DMBA)_4Cl_2$ (1). A round-bottom flask was charged with $Ru_2(OAc)_4Cl$ (0.474 g, 1.00 mmol), *N*,*N*′-dimethylbenzamidine (0.740 g, 5.00 mmol), LiCl (excess), Et_3N (2 mL), and 40 mL of THF. The mixture was gently refluxed for 2 h. After the removal of THF, the residue was dissolved in CH_2Cl_2 and filtered through a short silica gel pad (2 cm). Further recrystallization from CH_2Cl_2/hexanes yields 0.786 g of dark brown crystalline material (91% based on Ru). Data for **1**: R_f (CH_2Cl_2/hexanes, v/v 1/1), 0.48. MS−FAB (*m*/*e*, based on ^{101}Ru): 861 [M^+]. Anal. for $C_{36}H_{44}Cl_2N_8Ru_2$ Found (Calcd): C, 50.60 (50.17); H, 5.17 (5.15); N, 12.78 (13.00); Cl, 8.20 (8.23). χ_{mol}(corrected) = 3.44×10^{-3} emu; $\mu_{eff} = 2.86\ \mu_B$.

Preparation of $Ru_2(DMBA)_4(C_2SiMe_3)_2$ (2a). To a 20 mL THF solution containing 3.0 mmol $HCCSiMe_3$ was added 1.9 mL BuLi (1.6 M in hexanes) at about −80 °C. The mixture was slowly warmed to room temperature and stirred for another 1 h to yield a slight yellow solution. The solution was added to a 40 mL THF solution of **1** (0.60 mmol, 0.517 g) at room temperature, and the mixture was stirred for 3 h, during which the solution became dark red. After the solvent removal, the residue was washed with copious amount of MeOH and hexanes and dried under dynamic vacuum overnight to yield 0.486 g of red powder (82%). Data for **2a**: R_f (EtOAc/hexanes, v/v 1/4; the same solvent combination is used for R_f determination thereafter), 0.79. Anal. for $C_{46}H_{62}N_8Si_2Ru_2 \cdot H_2O$ Found (Calcd): C, 55.09 (55.03); H, 6.22 (6.38); N, 11.10 (11.17). MS−FAB (*m*/*e*, based on ^{101}Ru): 986 [M^+]. ^{1}H NMR ($CDCl_3$): 7.45−7.35 (m, 12H, aromatic), 6.97−6.95 (m, 8H, aromatic), 3.21 (s, 24H, NC**H**$_3$), 0.03 (s, 18H, Si(C**H**$_3$)$_3$). ^{13}C NMR-($CDCl_3$, C≡C): 95.91, 131.42. IR, υ(C≡C)/cm^{-1}: 1999(s).

Attempt to Prepare $Ru_2(DMBA)_4(C_2SiMe_3)Cl$. To a 20 mL THF solution containing 0.40 mmol HC_2SiMe_3 was added 0.25 mL BuLi (1.6 M in hexanes) at about −80 °C. The mixture was slowly warmed to room temperature and stirred for another hour. Half of the slight yellow solution was transferred to a 20 mL THF solution of **1** (0.20 mmol, 0.165 g) at room temperature, and the mixture was stirred for 3 h. TLC analysis revealed the formation of **2a** and the presence of unreacted **1**.

Preparation of $Ru_2(DMBA)_4(C_2H)_2$ (2b) was undertaken using the same procedure as that for **2a** and replacing LiC_2SiMe_3 with NaC_2H. Yield: 0.430 g (85%). Compound **2a** was the only Ru_2 species present after a THF solution containing both Bu_4NF and **2a** in 1:1 molar ratio was stirred at room temperature for 3 days. Replacing Bu_4NF with K_2CO_3 also failed to desilylate **2a** under the same conditions. Data for **2b**: R_f 0.67. Anal. for $C_{40}H_{46}N_8Ru_2 \cdot 2C_4H_8O$ Found (Calcd): C, 58.19 (58.52); H, 6.11 (6.34); N, 11.64 (11.38). MS−FAB (*m*/*e*, based on ^{101}Ru): 842 [MH^+]. ^{1}H NMR ($CDCl_3$): 7.45−7.40 (m, 12H, aromatic), 7.00−6.95 (m, 8H, aromatic), 3.24 (s, 24H, NC**H**$_3$), 2.26 (s, 2H, CC**H**). ^{13}C NMR-($CDCl_3$, C≡C): 58.84, 106.73. IR, υ(C≡C)/cm^{-1}: 1937(s).

Preparation of $Ru_2(DMBA)_4(C_2Ph)_2$ (2c) was undertaken using the same procedure as **2a** and replacing LiC_2SiMe_3 with LiC_2Ph. Yield: 0.567 g (95%). Data for **2c**: R_f, 0.67. Anal. for $C_{52}H_{54}N_8Ru_2$ Found (Calcd): C, 62.61 (62.88); H, 5.51 (5.48); N, 10.89 (11.28). MS−FAB (*m*/*e*, based on ^{101}Ru): 994 [MH^+]. ^{1}H NMR ($CDCl_3$): 7.40−7.31 (m, 12H, aromatic), 7.10−6.80 (m, 18H, aromatic), 3.23 (s, 24H, NC**H**$_3$). ^{13}C NMR($CDCl_3$, C≡C): 64.13, 120.92. IR, υ(C≡C)/cm^{-1}: 2080(s).

Preparation of $Ru_2(DMBA)_4(C_4SiMe_3)_2$ (3a) was undertaken using the same procedure as **2a** and replacing LiC_2SiMe_3 with LiC_4SiMe_3. Yield: 0.496 g (80%). Data for **3a**: R_f, 0.65. Anal. for $C_{50}H_{62}N_8Si_2Ru_2$ Found (Calcd): C, 58.07 (58.11); H, 5.91 (6.05); N, 10.75 (10.84). MS−FAB (*m*/*e*, based on ^{101}Ru): [MH^+]. ^{1}H NMR ($CDCl_3$): 7.45−7.38 (m, 12H, aromatic), 6.94−6.90 (m, 8H, aromatic), 3.19 (s, 24H, NC**H**$_3$), 0.09 (s, 18H, Si(C**H**$_3$)$_3$). ^{13}C NMR-($CDCl_3$, C≡C): 64.70, 67.22, 85.39, 105.02. IR, υ(C≡C)/cm^{-1}: 2107(s), 2165(m).

Preparation of $Ru_2(DMBA)_4(C_4H)_2$ (3b). $Ru_2(DMBA)_4(C_4SiMe_3)_2$ (0.104 g, 0.1 mmol) was dissolved in 20 mL of THF/MeOH (v:v = 3:1), to which 0.50 g K_2CO_3 was added. The mixture was stirred at room temperature until the complete consumption of the starting material was indicated by TLC (10 h). Removal of the solvent yielded the brownish-red residue, which was purified by washing with copious amount of MeOH to yield 0.084 g of analytically pure product (95%). Data for **3b**: R_f, 0.48. Anal. for $C_{44}H_{46}N_8Ru_2 \cdot 2CH_2Cl_2 \cdot C_6H_{14}$ Found (Calcd): C, 54.51 (54.54); H, 5.94 (5.63); N, 9.42 (9.79). MS−FAB (*m*/*e*, based on ^{101}Ru): 888 [M^+]. ^{1}H NMR ($CDCl_3$): 7.48−7.42 (m, 12H, aromatic), 7.00−6.95 (m, 8H, aromatic), 3.24 (s, 24H, NC**H**$_3$), 1.89 (s, 2H, CC**H**). ^{13}C NMR($CDCl_3$, C≡C): 65.53, 69.26, 93.48, 115.32. IR, υ(C≡C)/cm^{-1}: 2022(s), 2120(s).

X-ray Data Collection, Processing, and Structure Analysis and Refinement. Single crystals were grown via either a slow diffusion of hexanes into CH_2Cl_2 solution (**1**), slow evaporation of saturated hexanes/THF solution (**2a**), or slow cooling of saturated hexanes/ethyl acetate solution (**3b**). The X-ray intensity data were measured at 300 K on a Bruker SMART1000 CCD-based X-ray diffractometer system using Mo Kα (λ = 0.71073 Å). Thin plates of dimension $0.32 \times 0.22 \times 0.10$ mm^3 (**1**), $0.43 \times 0.30 \times 0.02$ mm^3 (**2a**), and $0.16 \times 0.16 \times 0.03$ mm^3 (**3b**) used for X-ray crystallographic analysis were cemented onto a quartz fiber with epoxy glue. Data were measured using ω scans of 0.3° per frame such that a hemisphere (1271 frames) was collected. No decay was indicated for any of three data sets by the recollection of the first 50 frames at the end of each data collection. The frames were integrated with the Bruker SAINT software package[33] using a narrow-frame integration algorithm, which also corrects for the Lorentz and polarization effects. Absorption corrections were applied using SADABS supplied by George Sheldrick.

The structures were solved and refined using the Bruker SHELXTL (Version 5.1) software package,[34−36] in the space groups *I*422, *Pbcn*, and $P2_1/n$ for crystals **1**, **2a**, and **3b**, respectively. Positions of all non-hydrogen atoms of diruthenium moieties were

(33) *SAINT V 6.035 Software for the CCD Detector System*; Bruker-AXS Inc.: Madison, WI, 1999.
(34) *SHELXTL 5.03 (WINDOW−NT Version), Program library for Structure Solution and Molecular Graphics*; Bruker-AXS Inc.: Madison, WI, 1998.
(35) Sheldrick, G. M. *SHELXS-90, Program for the Solution of Crystal Structures*; University of Göttigen: Göttigen, Germany, 1990.
(36) Sheldrick, G. M. *SHELXL-93, Program for the Refinement of Crystal Structures;* University of Göttigen: Göttigen, Germany, 1993.

Table 4. Crystal Data for Compounds **1**, **2a** and **3b**

	1·4THF	**2a**	**3b**
chemical formula	$C_{44}H_{44}N_8O_4Cl_2Ru_2$	$C_{46}H_{62}N_8Si_2Ru_2$	$C_{44}H_{46}N_8Ru_2$
fw	1021.9	985.4	889.0
space group	*I*422 (No. 97)	*Pbcn* (No. 60)	$P2_1/n$ (No. 14)
a, Å	14.070(1)	17.015(2)	12.539(1)
b, Å		13.976(2)	16.177(2)
c, Å	11.953(1)	21.518(2)	21.032(3)
β, deg			90.398(2)
V, Å^3	2366.3(4)	5098.7(9)	4265.9(9)
Z	2	4	4
T, °C	27	27	27
λ(Mo Kα), Å	0.71073	0.71073	0.71073
ρ_{calcd}, g cm^{-3}	1.434	1.284	1.384
μ, cm^{-1}	7.99	6.77	7.47
R	0.024	0.039	0.048
wR2	0.059	0.082	0.072

revealed by direct method. In the case of crystal **1**, the asymmetric unit contains only one-eighth of the molecule, which is related to the rest of the molecule via symmetry operations of D_4 point symmetry group with C_4 axis passing through Cl−Ru−RuA−ClA vector. One-fourth of a THF solvent molecule, possibly introduced from the synthesis, was also located in the asymmetric unit. In the case of **2a**, the asymmetric unit contains one-half of the molecule, which is related to the other half by a crystallographic 2-fold axis orthogonal to Ru1−Ru1A vector. In the case of **3b**, the asymmetric unit contains one diruthenium molecule. With all non-hydrogen atoms being anisotropic and all hydrogen atoms in calculated position and riding mode, the structure was refined to convergence by least-squares method on F^2, SHELXL-93, incorporated in SHELXTL.PC V 5.03. Relevant information on the data collection and the figures of merit of final refinement are listed in Table 4.

Acknowledgment. The generous support from both the University of Miami (start-up fund, the funding for the CCD-diffractometer, and a Maytag graduate fellowship to Mr. G.-L. Xu) and the Petroleum Research Fund/ACS (36595-AC3) are gratefully acknowledged.

Note Added after ASAP: The version of this article posted ASAP on May 23, 2002, contained an incorrect $E(-1/-2)$/V value for **3b** in Table 3. The correct value, −1.945, appears in the version posted on May 28, 2002.

Supporting Information Available: Scan-rate dependent CV study of compound **2b** (Figure S1) and X-ray crystallographic files in CIF format for the structure determination of compounds **1**, **2a**, and **3b**. This material is available free of charge via the Internet at http://pubs.acs.org.

IC0200794